The Journal of Neuroscience, August 1, 1999, *19*(15):6712–6722

Monoamine Control of the Pacemaker Kernel and Cycle Frequency in the Lobster Pyloric Network

Amir Ayali and Ronald M. Harris-Warrick

Section of Neurobiology and Behavior, Cornell University, Ithaca, New York 14853

The monoamines dopamine (DA), serotonin (5HT), and octopamine (Oct) can each sculpt a unique motor pattern from the pyloric network in the stomatogastric ganglion (STG) of the spiny lobster *Panulirus interruptus.* In this paper we investigate the contribution of individual network components in determining the specific amine-induced cycle frequency. We used photoinactivation of identified neurons and pharmacological blockade of synapses to isolate the anterior burster (AB) and pyloric dilator (PD) neurons. Bath application of DA, 5HT, or Oct enhanced cycle frequency in an isolated AB neuron, with DA generating the most rapid oscillations and Oct the slowest. When an AB–PD or AB–2xPD subnetworks were tested, DA often reduced the ongoing cycle frequency, whereas 5HT and Oct both evoked similar accelerations in cycle frequency. However, in the intact pyloric network, both DA and Oct either reduced or did not alter the cycle frequency, whereas 5HT continued to enhance the cycle frequency as before. Our results show that the major target of 5HT in altering the pyloric cycle frequency is the AB neuron, whereas DA's effects on the AB–2xPD subnetwork are critical in understanding its modulation of the cycle frequency. Octopamine's effects on cycle frequency require an understanding of its modulation of the feedback inhibition to the AB–PD group from the lateral pyloric neuron, which constrains the pacemaker group to oscillate more slowly than it would alone. We have thus demonstrated that the relative importance of the different network components in determining the final cycle frequency is not fixed but can vary under different modulatory conditions.

Key words: central pattern generation; neuromodulation; pacemaker neurons; stomatogastric ganglion; pyloric network; dopamine; serotonin; octopamine

Control of cycle frequency is one of the most important parameters for the actions of neuromodulators on rhythmic motor patterns such as locomotion, mastication, and ventilation. Cycle frequency is determined by neuronal interactions within the central pattern generator (CPG) networks that organize rhythmic movements (Getting, 1989). Two main mechanisms for alteration of cycle frequency have been described (Stein et al., 1998, Katz, 1999): alteration of intrinsic properties of critical pacemaker neurons (for review, see Selverston et al., 1998) and modulation of the strength of synaptic connections between the CPG network neurons (Sillar et al., 1998). The relative importance of these two mechanisms in setting the cycle frequency is difficult to determine in complex systems.

The pyloric circuit in the lobster stomatogastric ganglion (STG) provides a unique opportunity to study how the various targets of a neuromodulator contribute to the network's final cycle frequency. Traditionally (Miller, 1987; Johnson and Hooper, 1992), the rapidly oscillating anterior burster (AB) interneuron is thought to be the most important cell for determining the pyloric cycle frequency. However, a number of other network neurons are known to contribute to the generation of the final pyloric cycle frequency. It has long been known from both experimental and theoretical studies that the electrically coupled pyloric dilator (PD) neurons are instrumental in shaping the rhythm (Marder, 1984; Eisen and Marder, 1984; Hooper and Marder, 1987; Kepler et al., 1990; Abbott et al., 1991). Hence, the AB–PD subnetwork is typically referred to as the pacemaker kernel of the network. This subnetwork receives inhibitory feedback from the lateral pyloric (LP) neuron (to the PD neurons) (Fig. 1), and Selverston and Miller (1980) reported that inactivation of the LP neuron results in an increase in the spontaneous pyloric cycle frequency. Finally, the ventricular dilator (VD) neuron makes rectifying electrical synapses with both the AB and PD neurons (Fig. 1) (Johnson et al., 1993) and in theory could function to enhance the repolarization of the pacemaker neurons leading to the next burst.

Much is known about the characteristics of the individual component neurons and synapses of the pyloric network (Eisen and Marder, 1982; Miller and Selverston, 1982a,b; Hartline and Graubard, 1992; Baro et. al, 1997) and how they are affected by neuromodulators (Dickinson et al., 1990; Harris-Warrick and Marder, 1991; Marder et al., 1994; Harris-Warrick et al., 1995a,b; Johnson and Harris-Warrick, 1997; Ayali and Harris-Warrick, 1998; Kloppenburg and Harris-Warrick, 1999). A main advantage of the pyloric network is the ability to study isolated subsets of neurons, through pharmacological blockade of synapses (Bidaut, 1980) and photoinactivation to eliminate individual neurons (Fig. 1) (Miller and Selverston, 1979; Selverston and Miller, 1980). Practically all the cellular and synaptic components of the pyloric network are targets of monoamine modulation: dopamine (DA), octopamine (Oct), and serotonin (5HT) have been found to have a bewildering variety of effects on the intrinsic electrical properties of all pyloric neurons, as well as on synaptic transmission between network members (Flamm and Harris-Warrick, 1986a,b; Harris-Warrick and Flamm, 1986, 1987; Harris-Warrick et al.,

Received Jan. 12, 1999; revised April 28, 1999; accepted May 3, 1999.

This work was supported by National Institutes of Health Grant NS17323. We thank Dr. P. Meyrand for his valuable comments on an early version of this manuscript.

Correspondence should be addressed to Amir Ayali at his present address: Department of Zoology, Faculty of Life Sciences, Tel-Aviv University, Ramat-Aviv, Tel-Aviv, Israel 69978.

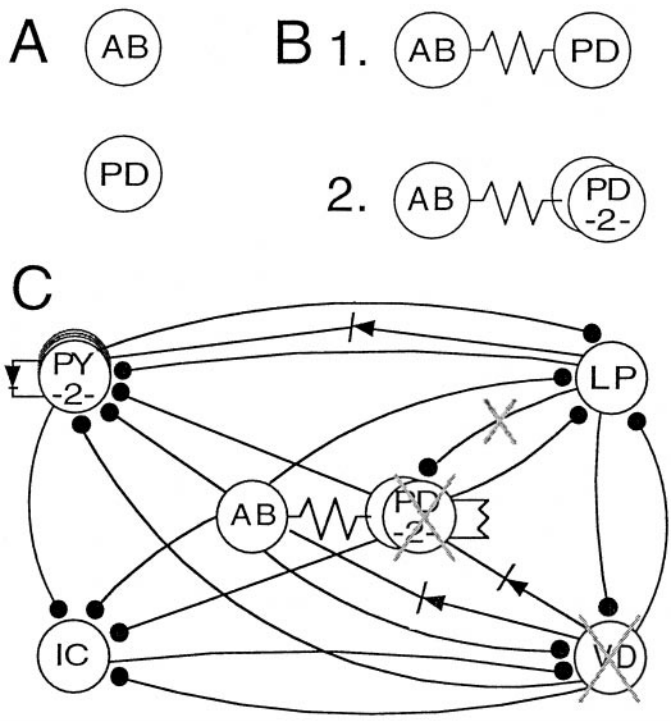

Figure 1. Schematic diagram of the different preparations used in this study. *A*, Isolated AB or PD neurons (descending modulatory inputs were either blocked by a tetrodotoxin block on the stomatogastric nerve or kept intact). *B*, An AB–PD (*1*) or AB–2xPD (*2*) pacemaker subnetwork (with or without descending inputs). *C*, The intact pyloric circuit (modulatory inputs were kept intact). An example of the method of isolating neurons and subnetworks is also shown in *C*. To isolate the AB–PD subnetwork (shown in *B1*), the VD neuron and one PD neuron were photoinactivated, and the LP → PD synapse was pharmacologically blocked with picrotoxin. All synaptic connections are either electrical (nonrectifying synapses, resistors; rectifying synapses, diodes) or chemical inhibitory (*small circles*).

1995a,b; Johnson et al., 1995; Johnson and Harris-Warrick, 1997; Ayali et al., 1998).

Now that amine effects on individual components of the circuit have been mapped, the next goal is to try to put the system back together. In this paper we show that the effects of DA, 5HT, and Oct on the pyloric cycle frequency depend critically on interactions within the traditional pacemaker group as well as on synaptic interactions in the pyloric network. Thus, the network components that determine the final cycle frequency vary depending on the different modulatory conditions.

MATERIALS AND METHODS

Animals. Pacific spiny lobsters (*Panulirus interruptus*) of both sexes weighing between 0.5 and 1 kg were purchased from Don and Laurice Tomlinson (San Diego, CA), and maintained in marine aquaria at 15–16°C until use.

Saline and chemicals. Panulirus saline was composed of (in mM): NaCl 479, KCl 12.8, $CaCl_2$ 13.7, Na_2SO_4 3.9, $MgSO_4$ 10.0, glucose 2.0, Tris base 11.1, maleic acid 5.1, pH 7.4–7.6 (Mulloney and Selverston, 1974). All salts and drugs were obtained from Sigma (St. Louis, MO).

Physiology. The stomatogastric nervous system was dissected as described by Selverston et al. (1976) and placed in a preparation dish filled with *Panulirus* saline. The STG was desheathed, enclosed in a small (1 ml) pool of saline walled by Vaseline, and constantly superfused at 3 ml/min with oxygenated saline at 16–17°C. The cell bodies of the pyloric neurons were identified by correlation of action potentials recorded intracellularly in the soma and extracellularly on identified motor nerves, and by the characteristic shape and timing of bursts of action potentials in the pyloric rhythm. Extracellular recordings were made with bipolar stainless-steel pin electrodes. Standard intracellular techniques were used for voltage recordings using KCl-filled (3 M, 15–25 MΩ) microelectrodes. The AB–2xPD subnetwork was isolated by photoinactivation (Miller and Selverston, 1979) of the VD neuron in addition to pharmacological blockade (10^{-5} M picrotoxin) of the LP → PD synapse (Fig. 1). Further inactivation of one PD neuron generated the AB–PD subnetwork. Single neurons were isolated by additional photoinactivation of the remaining PD or AB neuron. Amine solutions were prepared in normal saline just before bath application. As in earlier studies (Flamm and Harris-Warrick, 1986a,b; Johnson and Harris-Warrick, 1990), we used 10^{-4} M DA, 10^{-5} M 5HT, and 10^{-4} M to 10^{-5} M Oct. When required, inputs to the STG from higher ganglia were blocked by applying 10^{-7} M tetrodotoxin (TTX) saline to a small pool walled with Vaseline on the desheathed stomatogastric nerve. This stopped rhythmic activity of the pyloric network (Russell, 1979; Nagy and Miller, 1987).

Statistical significance was tested and stated when $p < 0.05$ (two-tailed *t* test for unpaired or paired variates, as was appropriate).

RESULTS

Amine modulation of the isolated AB or PD neurons

The modulatory effects of the monoamines on isolated pyloric neurons have been studied previously (Flamm and Harris-Warrick, 1986a,b; Harris-Warrick and Flamm, 1987; Harris-Warrick et al., 1995a,b; Kloppenburg et al., 1999). In these studies, all descending inputs to the pyloric network were blocked to test amine effects on the isolated neurons in a basal, nonmodulated state. Because the pyloric pacemaker neurons are conditional oscillators, blocking modulatory inputs results in a baseline condition of nonoscillating neurons with no ongoing pyloric rhythm (Nagy and Miller, 1987). In the present study, we confirmed these previous results, and in addition we studied amine modulation of the AB and PD neurons when isolated from other pyloric neurons but with intact descending modulatory inputs.

The two experiments shown in Figure 2*A* demonstrate the effects of bath-applied amines on the isolated AB and PD neurons. As described previously (Flamm and Harris-Warrick, 1986b; Harris-Warrick and Flamm, 1987), after blocking descending modulatory inputs the AB neuron was in a quiescent nonoscillatory state, and all three amines had excitatory effects to induce AB rhythmic bursting (Fig. 2*A1*). Dopamine was the most potent excitatory modulator, inducing the largest oscillations with the most spikes at the highest cycle frequency; 5HT was intermediate, and Oct had the weakest excitatory effects (Figs. 2*A1*, 3*A*).

The AB neuron with intact modulatory descending inputs was bursting rhythmically (Fig. 2*B1*). The modulatory effects of the amines under these conditions were qualitatively similar to those seen in the blocked preparation (Fig. 2, compare *A*, *B*). Although not all differences between the effects of the three amines were statistically significant (mainly because of a large variation in control cycle frequencies), some trends were very clear. Dopamine induced the highest AB cycle frequency, number of spikes per burst, and spike frequency within an AB neuron burst (Fig. 3). Dopamine also generated the largest amplitude oscillations in the AB neuron (Fig. 2). Octopamine had the weakest enhancement of cycle frequency, had very minor effects on the AB neuron's spiking, and generated no net enhancement of the AB neuron oscillation amplitude (14.7 ± 7.5 and 14.4 ± 4.5 mV in control and Oct conditions, respectively, compared with 18.7 ± 5.0 mV in DA; $n = 5$). Serotonin had intermediate effects on all these parameters.

As shown previously (Flamm and Harris-Warrick, 1986b), the isolated PD neuron with no modulatory inputs fired tonically and was strongly inhibited by DA (Fig. 2*A2*). Dopamine caused a hyperpolarization of 7.2 ± 1.8 mV ($n = 10$) and abolished the PD

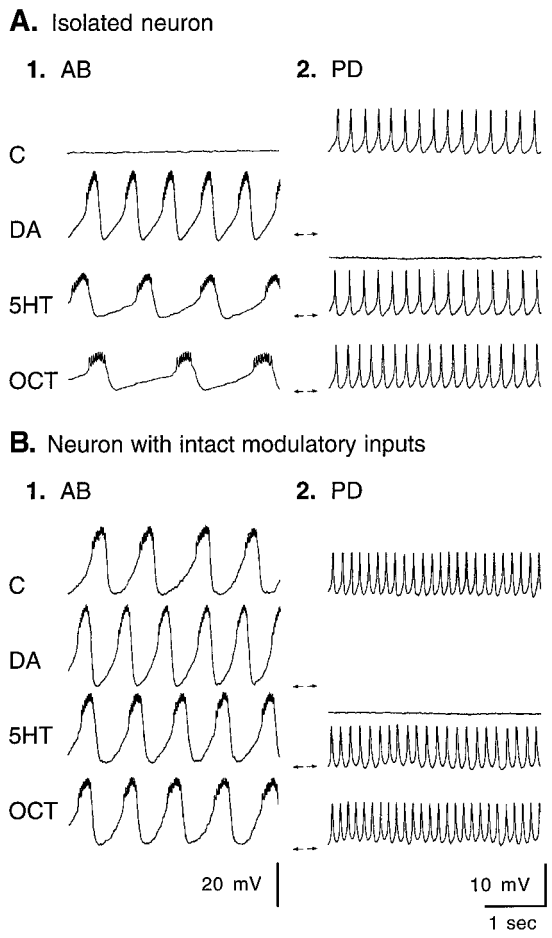

Figure 2. Effects of bath-applied amines on the AB and PD neurons. Each neuron was isolated from all pyloric synaptic inputs as described in Materials and Methods. Descending modulatory inputs via the stomatogastric nerve were either blocked (*A*) or kept intact (*B*). Both *A1* and *B1* for the AB neuron, as well as *A2* and *B2* for the PD neuron, show recordings from a single neuron. Dopamine (*DA*), serotonin (*5HT*), and octopamine (*OCT*) induced fully reversible changes in the cellular activity. The control resting membrane potential or potential at the lowest voltage of oscillations is marked by *arrows*.

neuron's tonic firing. Octopamine had a slight but not statistically significant excitatory effect, whereas 5HT had no detectable effect on the PD neuron's spontaneous firing properties (Fig. 2*A2*). When modulatory inputs from other ganglia are intact, the isolated PD neurons are sometimes capable of generating bursting pacemaker potentials (R. Elson, personal communication). However, in 80% of our experiments with intact descending modulatory inputs, the isolated PD neuron fired tonically (Fig. 2*B2*), with only small and slow membrane potential oscillations (up to 1 mV, 0.2 Hz), which caused only subtle changes in tonic spike frequency (data not shown). These slow oscillations in the PD neuron's membrane potential were never seen after blocking descending inputs. The PD neuron spike frequency was higher with intact descending modulatory inputs than in the isolated state (6.8 ± 1.2 Hz compared with 4.2 ± 0.3 Hz, respectively; $n = 5$) (see also Fig. 2). As seen in Figure 2, the amines' effects on the PD neuron firing properties were essentially the same in the presence of descending modulatory inputs (Fig. 2*B2*) as in the isolated PD neuron (Fig. 2*A2*): DA abolished PD neuron activity, whereas 5HT had no effect and Oct weakly enhanced tonic spike activity.

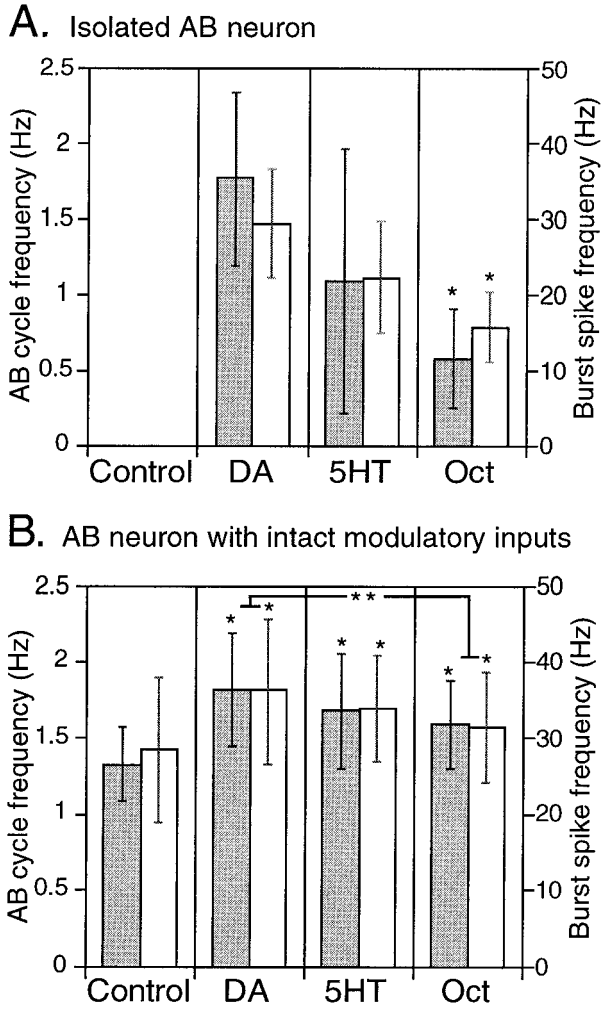

Figure 3. Effects of bath-applied dopamine (*DA*), serotonin (*5HT*), and octopamine (*Oct*) on the AB neuron, when isolated from all pyloric synaptic inputs as described in Materials and Methods, with descending modulatory inputs in the stomatogastric nerve blocked (*A*) or left intact (*B*). *Filled bars*, AB cycle frequency; *open bars*, mean spike frequency within the AB burst. The data show the mean of three (*A*) or five (*B*) different preparations ± SD. In *A*, both parameters measured in Oct (*) are significantly different from DA and 5HT frequencies. Both parameters measured in all three amines in *B* (*) are significantly different from control. In addition, the measurements in Oct are significantly different from those in DA (**).

Amine modulation of the AB–PD and AB–2xPD subnetworks

When isolated from all descending inputs, the AB–PD subnetwork did not show oscillatory behavior; the PD neuron fired tonically, whereas the AB neuron was silent. Because DA, Oct, and 5HT all evoke rhythmic oscillations in an isolated AB neuron, we expected the amines to activate synchronized cycling in the AB–PD subnetwork, and this was indeed observed. The DA-evoked cycling in the AB–PD subnetwork (0.9 ± 0.4 Hz; $n = 8$) was significantly slower then DA-evoked cycling in the isolated AB neuron (1.8 ± 0.6 Hz; $n = 5$). 5HT-evoked cycling was similar in both cases (0.9 ± 0.4 Hz for AB–PD vs 1.1 ± 0.5 Hz for AB; $n = 5$), whereas Oct-evoked cycling was significantly faster in the AB–PD subnetwork (0.9 ± 0.3 Hz; $n = 5$) than in the isolated AB neuron (0.6 ± 0.3 Hz; $n = 5$).

In an AB–PD subnetwork with intact modulatory inputs, both

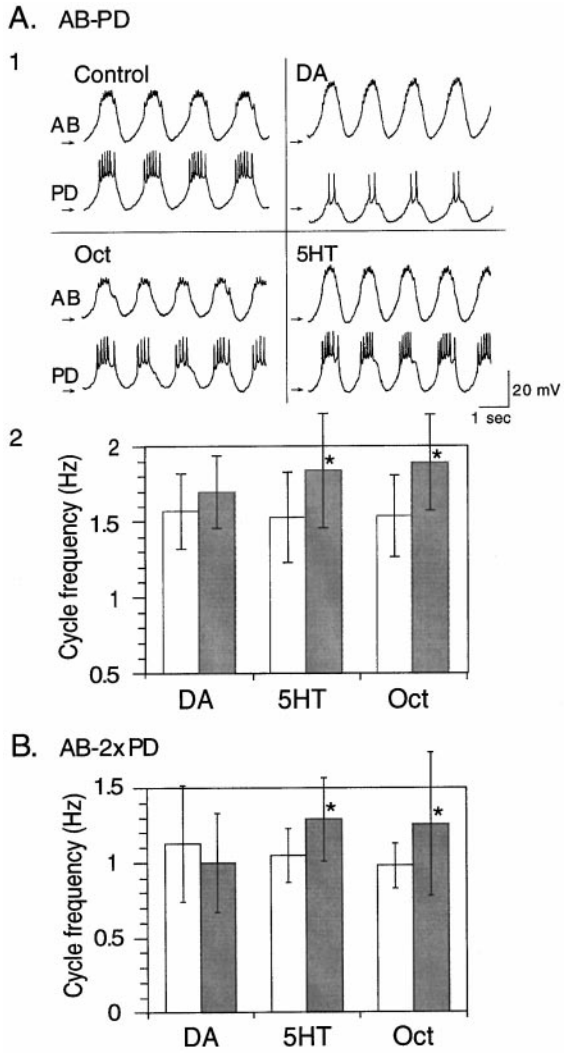

Figure 4. *A*, Effects of bath-applied amines on an AB–PD subnetwork isolated from all pyloric synaptic inputs. Descending modulatory inputs were kept intact. *A1*, Simultaneous recordings from the AB and PD neurons. The recordings shown in all panels are from a single preparation. Dopamine (*DA*), octopamine (*Oct*), and serotonin (*5HT*) induced fully reversible and reproducible changes in the subnetwork activity. The control oscillation trough membrane potential of both neurons is marked by *arrows* in all panels. *A2*, Effects of the bath-applied amines on cycle frequency in the AB–PD subnetwork. *Open bars*, Control; *filled bars*, amine bath application. *B*, Effects of bath-applied amines on cycle frequency in an AB–2xPD subnetwork, with descending modulatory inputs intact. In *A2* and *B*, data show the mean of five to eight different preparations ± SD. Cycle frequencies in 5HT and Oct (*) are significantly different from control and DA but not from each other.

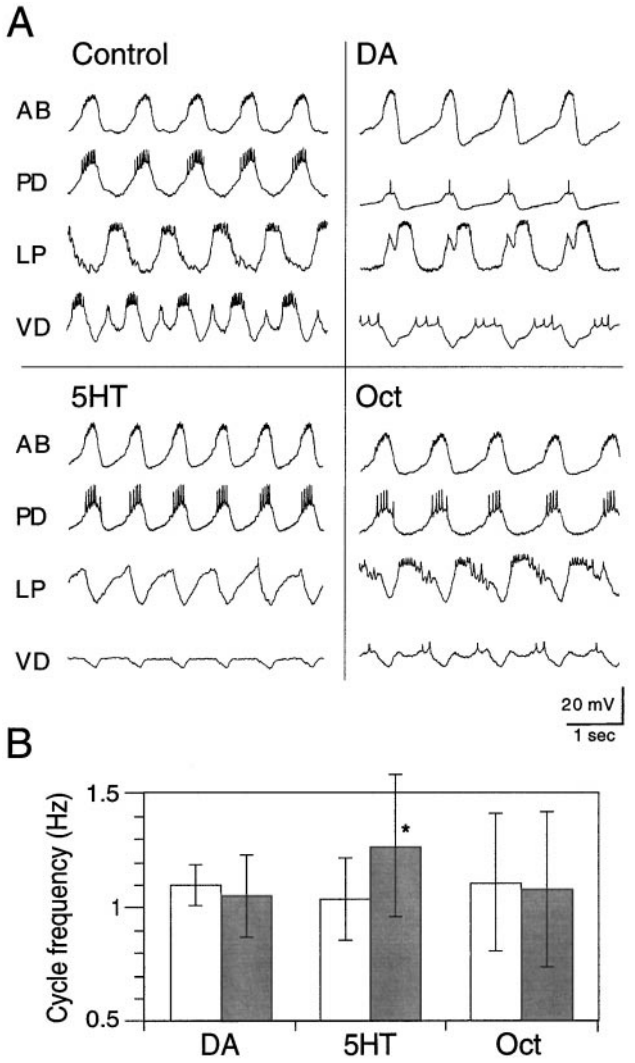

Figure 5. Effects of bath-applied dopamine (*DA*), serotonin (*5HT*), and octopamine (*Oct*) on the intact pyloric network with descending modulatory inputs. *A*, Simultaneous recordings from four of the six pyloric neuron classes. All of the recordings are from a single preparation. All amine effects were reversible after wash with normal saline. *B*, Effects of bath-applied amines on the pyloric cycle frequency in the intact pyloric network with descending modulatory inputs. *Open bars*, Control; *filled bars*, amine bath application. Data show the mean of six different preparations ± SD. Cycle frequency in 5HT (*) is significantly different from control, Oct, and DA frequencies.

neurons oscillate synchronously without amine addition, reflecting the strong electrical coupling between them (Fig. 4*A*, *Control*) (Miller, 1987). Figure 4*A* shows an example of the modulatory effects of the three amines on an AB–PD subnetwork with intact descending inputs. Some of the amine modulatory effects on the AB and PD neurons' firing properties were qualitatively similar to the effects on the isolated neurons (Figs. 2*B*, 3*B*). For example, DA inhibited PD neuron spiking while generating higher amplitude oscillations in the AB neuron. The amplitude of the AB neuron oscillations as well as other AB firing characteristics were intermediate in 5HT and smallest in Oct (data not shown). However, looking at the amine effects on cycle frequency of the two-cell subnetwork reveals a different picture. The major result is that although the order of cycle frequencies in the isolated AB neuron was DA > 5HT > Oct (Fig. 3) (Flamm and Harris-Warrick, 1986b), this order changes in the AB–PD subnetwork with descending modulatory inputs to Oct = 5HT > DA (Fig. 4*A*). Thus, DA switched position from evoking the fastest cycle frequency in the isolated AB neuron to the slowest cycle frequency in the AB–PD subnetwork.

The basic features of the AB–PD subnetwork amine-induced rhythms are also seen in a pacemaker subnetwork with two PD neurons (Fig. 4*B*). Two major differences are seen. First, the control cycle frequency (without amines) is somewhat lower with two PD neurons, reflecting the electrical drag the PD neurons exert on the AB oscillator (Kepler et al., 1990; Sharp et al., 1992). Second, the effect of DA is changed from a modest enhancement

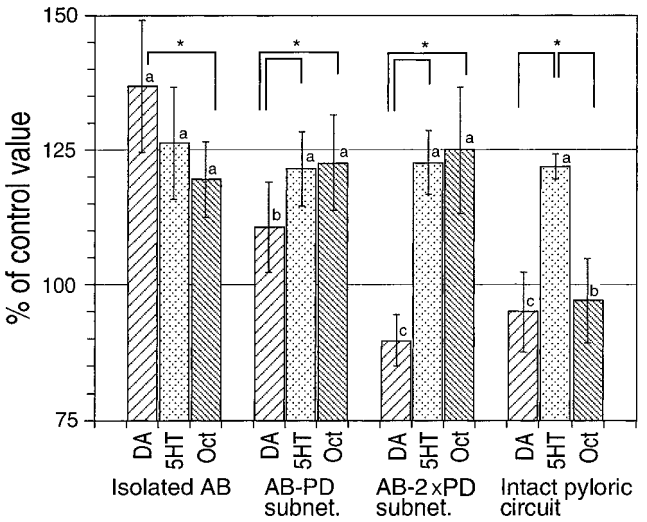

Figure 6. Summary of amine effects on the cycle frequency of an isolated AB neuron, an AB–PD subnetwork, an AB–2xPD subnetwork, and an intact pyloric circuit, all with intact descending modulatory inputs. Data shown as percentage relative to control frequencies in each condition. Means of five to eight different preparations ± SEM are shown. An *asterisk* signifies a significant difference between amines within the same type of preparation. For each amine, *bars* marked by a *different letter* show statistically significant difference between a single amine-induced change in the different types of preparations; the *same letter* indicates no significant difference between the different types of preparations.

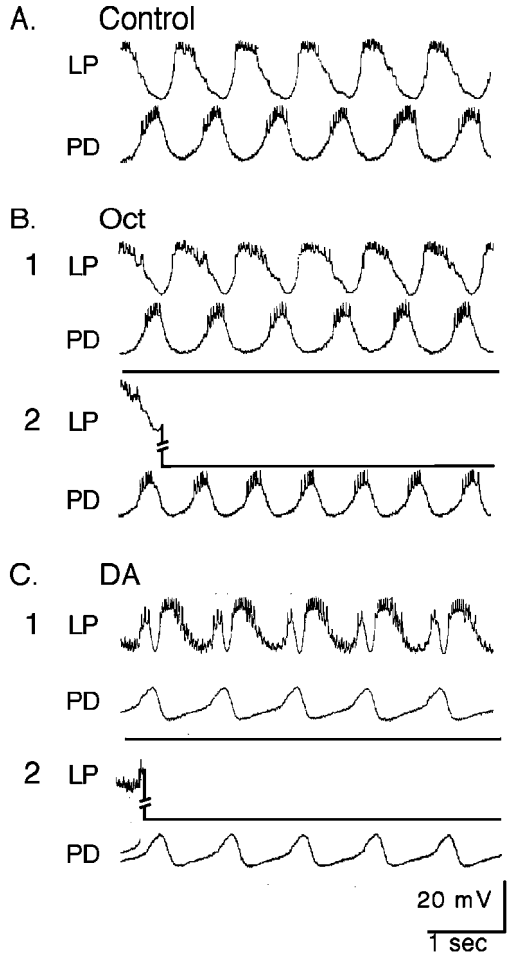

Figure 7. The effect of the LP neuron on octopamine (*Oct*) and dopamine (*DA*) induced rhythms in an intact pyloric network with descending modulatory inputs. Simultaneous recordings from the LP and a PD neuron in control conditions (*A*), during Oct bath application (*B*), and during DA bath application (*C*) are shown. In both Oct and DA, the traces shown in *1* demonstrate the final and stable amine-induced rhythm (~5 min of bath application). The traces in *2* show the effect of strongly hyperpolarizing the LP neuron by current injection on the amine-induced rhythm. The traces shown in *2* were recorded a few seconds after the recordings shown in *1*. The amine effects and effects of hyperpolarizing the LP neuron were fully reversible.

of cycle frequency in the AB–PD subnetwork to a consistent although small reduction in cycle frequency of the AB–2xPD subnetwork. Thus, as we add to the AB neuron the first and then the second PD neuron, the opposing effects of DA on the two cell types add up to change the DA modulatory effect from strong excitation to slight inhibition. This point will be further dealt with below. The enhancement of cycle frequency by 5HT and Oct is essentially the same in AB–PD and AB–2xPD subnetworks (Fig. 4, compare *A*, *B*).

Amine modulation of the intact pyloric network with descending modulatory inputs

Having established how the amines determine the cycle frequency of the AB–PD pacemaker subnetworks, we wished to compare these results with the intact pyloric network to investigate whether the AB–PD pacemaker group alone performs the final determination of the pyloric cycle frequency. Figure 5*A* shows a simultaneous recording from four of the pyloric cell types in an intact pyloric network with descending modulatory inputs. This figure shows a typical example of the nature of the amine effects. Dopamine somewhat reduced the pyloric cycle frequency, 5HT had a strong excitatory effect, and Oct slightly decreased the ongoing cycle frequency. In other examples where the pyloric constrictor (PY) neurons fired less strongly during Oct superfusion and thus did not confine the Oct-induced prolongation of the LP burst, the inhibitory effect of Oct was even stronger. On averaging the responses in six intact preparations (Fig. 5*B*), 5HT evoked a significant increase in cycle frequency, to essentially the same extent as its effects in the AB neuron and the AB–PD subnetworks. Dopamine's slight reduction of cycle frequency in the intact network also resembles its effects on the AB–2xPD subnetwork (Fig. 4*B*). However, the effects of Oct on the intact network are very different from its effects on the more reduced subnetworks: instead of enhancing the cycle frequency, Oct caused the cycle frequency to be virtually unchanged or even decreased.

Figure 6 summarizes all the amine effects on cycle frequency as we advance from the single AB neuron up to the intact pyloric network. Dopamine evoked the highest change in cycle frequency in the isolated AB neuron but the lowest change in the AB–PD subnetworks and the intact network. Octopamine and 5HT evoked similar changes in cycle frequencies in the isolated AB neuron and had practically identical effects in the AB–PD as well as AB–2xPD subnetworks. However, these amines' effects on the full circuit were quite different: 5HT continued to enhance cycle frequency to the same extent as in the simpler preparations, whereas Oct did not significantly alter cycle frequency above control values.

These changes in Oct's effects in the intact pyloric network must reflect different contributions of other members of the pyloric circuit that provide feedback to the AB–PD group. The two inputs to the pyloric pacemaker neuron group from the rest

of the network are the chemical inhibitory synapse from the LP neuron to the PD neurons, and the VD neuron's rectifying electrical coupling to the AB and PD neurons (Fig. 1). A close look at the traces in Figure 5*A* suggests that the differences in Oct's effects on cycle frequency in the pacemaker and intact networks (Fig. 6) are attributable primarily to the LP neuron's inhibition of the PD neurons in the intact circuit. The LP neuron burst duration is extended during Oct application (Fig. 5) (Flamm and Harris-Warrick, 1986a). Octopamine also enhances synaptic transmission in the LP → PD inhibitory synapse (Johnson et al., 1995). The LP neuron's graded inhibition and spike-evoked inhibitory postsynaptic potentials can be seen in the PD neuron traces.

On the basis of these results, we hypothesized that in the presence of Oct, LP inhibition of the PD neuron delays the rise of the next burst in the pacemaker neurons, thus slowing the rhythm. We tested the role of LP neuron inputs in shaping the amine-induced rhythms by temporarily removing LP inhibition of the PD neurons during amine bath application. This was done by strongly hyperpolarizing the LP neuron to approximately −100 mV by current injection. Figure 7 shows that Oct enhanced the burst duration of the LP neuron, but the Oct-evoked cycle frequency (Fig. 7*B1*) (1.24 Hz) did not change from its control value (Fig. 7*A*) (1.20 Hz). When the LP neuron was hyperpolarized to remove its inhibition of the pacemaker neuron group (via the PD neurons), a significant enhancement of the cycle frequency occurred (Fig. 7*B2*) (1.50 Hz; on average 15.1 ± 3.3% change from before LP hyperpolarization; $n = 7$). This suggests that LP inhibition constrains the AB–PD group to oscillate at a lower frequency than it would without the LP input during Oct superfusion.

We repeated this test with all three amines in the same preparation. LP neuron hyperpolarization had practically no effect on the 5HT-induced cycle frequency (data not shown) (1.5 ± 0.8% change from control frequency; $n = 3$). In contrast to Oct, 5HT directly inhibits the LP neuron (Fig. 5*A*)(Flamm and Harris-Warrick, 1986a,b); it also weakens LP output synapses (Johnson et al., 1995), thus reducing the impact of the LP neuron's inhibition of the pacemaker group. As a result, 5HT modulation of cycle frequency in the AB–2xPD subnetwork and the intact circuit is very similar (Fig. 6). Dopamine very strongly excites the LP neuron even more than Oct (Figs. 5*A*, 7*C*) (Harris-Warrick et al., 1995b) and also strengthens LP output synapses (Johnson et al., 1995), and we would thus expect the removal of the LP inhibition by hyperpolarization to speed up the cycle frequency during DA. However, as seen in Figure 7*C*, LP neuron hyperpolarization had no effect on the DA-induced rhythm (Fig. 7*C2*) (1.1 ± 2.3% change from control frequency; $n = 7$), and the LP neuron does not seem to play a significant role in determining the pyloric cycle frequency during DA application.

Careful examination of Figure 5 suggests that the effectiveness of LP feedback inhibition of the AB–PD group depends not only on the amplitude of the inhibition but also on its phasing; that is, exactly when in the cycle the LP neuron inhibition of the PD neuron (and thus AB) occurs (Flamm and Harris-Warrick, 1986a; Ayali and Harris-Warrick, 1998). Under control conditions, the LP neuron delivers a moderate but brief (~200 msec at 1 Hz cycle frequency) inhibition starting shortly after the middle of the cycle between AB–PD bursts. In the presence of DA, the LP neuron is highly excited to deliver a much stronger inhibition of similar duration (~200 msec), but at an earlier phase (~0.35) in the cycle. In contrast, during Oct application, the LP neuron is excited to an intermediate level but fires a much longer burst (~400 msec), starting at a phase similar to control (~0.5) and lasting much longer.

To study these parameters further, we eliminated the inhibitory LP → PD synapse by pharmacological blockade and mimicked it by intracellular hyperpolarizing current injections to one of the PD neurons while monitoring its membrane potential with a second electrode (Fig. 8). We used three different current injection protocols to hyperpolarize the PD neuron: a short mild inhibition (200 msec, 0.2 nA) to mimic LP inhibition in control conditions, a long, slightly stronger injection (400 msec, 0.4 nA) to mimic Oct conditions, and a short but strong inhibition (200 msec, 0.6 nA) to mimic DA conditions. In this experiment we did not add the amines, so that we could isolate the effects of the three different inhibitory inputs to the PD neuron on the cycle frequency. Figure 8*A* demonstrates the effects of the current injections mimicking the LP inhibition during DA and Oct. Although the DA-like inhibition is stronger, it has no effect on the cycle frequency, whereas the longer-lasting although weaker Oct-like inhibition causes a significant prolongation of the cycle period. To determine whether the major difference between the LP inputs in DA and Oct conditions is the phase of the inhibition, we tested the effect of the three types of stimuli at different stimulus phases. Figure 8*B* shows these results. The *y*-axis shows the period of the cycle that included current injection as a percentage of the cycle preceding it, which had no injection (as seen in Fig. 8*A*), and the *x*-axis gives the phase of the end of the current injection pulse, again as a fraction of the preceding cycle, which had no current injection (thus the end phase could be greater than one, as for example in the sweep marked Oct in Fig. 8*A*).

Figure 8*B* shows two major findings. First, all three stimulus protocols were capable of generating a significant change in cycle period (up to 25%). The most important parameter was indeed phase of the stimulus, specifically the end of the stimulus. As shown by the linear fit, terminating the inhibition at a phase later then 0.8 caused a delay in the rise of the next pacemaker burst and a prolongation of the period. The second point is that the combination of stimulus intensity, duration, and phase that best mimicked the LP inhibition under control, DA, or Oct conditions also generated an effect or lack of effect on cycle period similar to that shown in the corresponding experimental conditions. Control-like injections (Fig. 8*B*, *open squares*) with normal termination phases of 0.75–0.85 (Ayali and Harris-Warrick, 1998) did not greatly alter the pyloric cycle period. Stronger, DA-like injections (Fig. 8*B*, *black squares*) that mimic the LP phase advance to terminate at phases of 0.55–0.65 (Harris Warrick et al., 1995a; Ayali and Harris-Warrick, 1998) also had little effect on the cycle period or caused a slight shortening, consistent with the slightly higher DA-induced cycle frequency of the intact pyloric network relative to the AB–2xPD subnetwork (Fig. 6). Longer lasting, Oct-like injections (Fig. 8*B*, *gray squares*) with delayed termination phases of 1.05–1.15 (Flamm and Harris-Warrick, 1986a) caused a significant prolongation of the cycle. Again, this mimics Oct's reduction of cycle frequency of the intact network compared with the AB–2xPD subnetwork (Fig. 6). Finally, it was possible to entrain an ongoing pyloric rhythm to the cycle frequencies corresponding to the control, DA, or Oct conditions by repetitive stimulation, using the specific control-, DA-, or Oct-like current injection parameters (Fig. 8*C*). Strong repetitive stimulation at an early phase (mimicking DA conditions) had a very minor or no effect on cycle frequency compared with the control, whereas prolonged weaker inhibition at a later phase

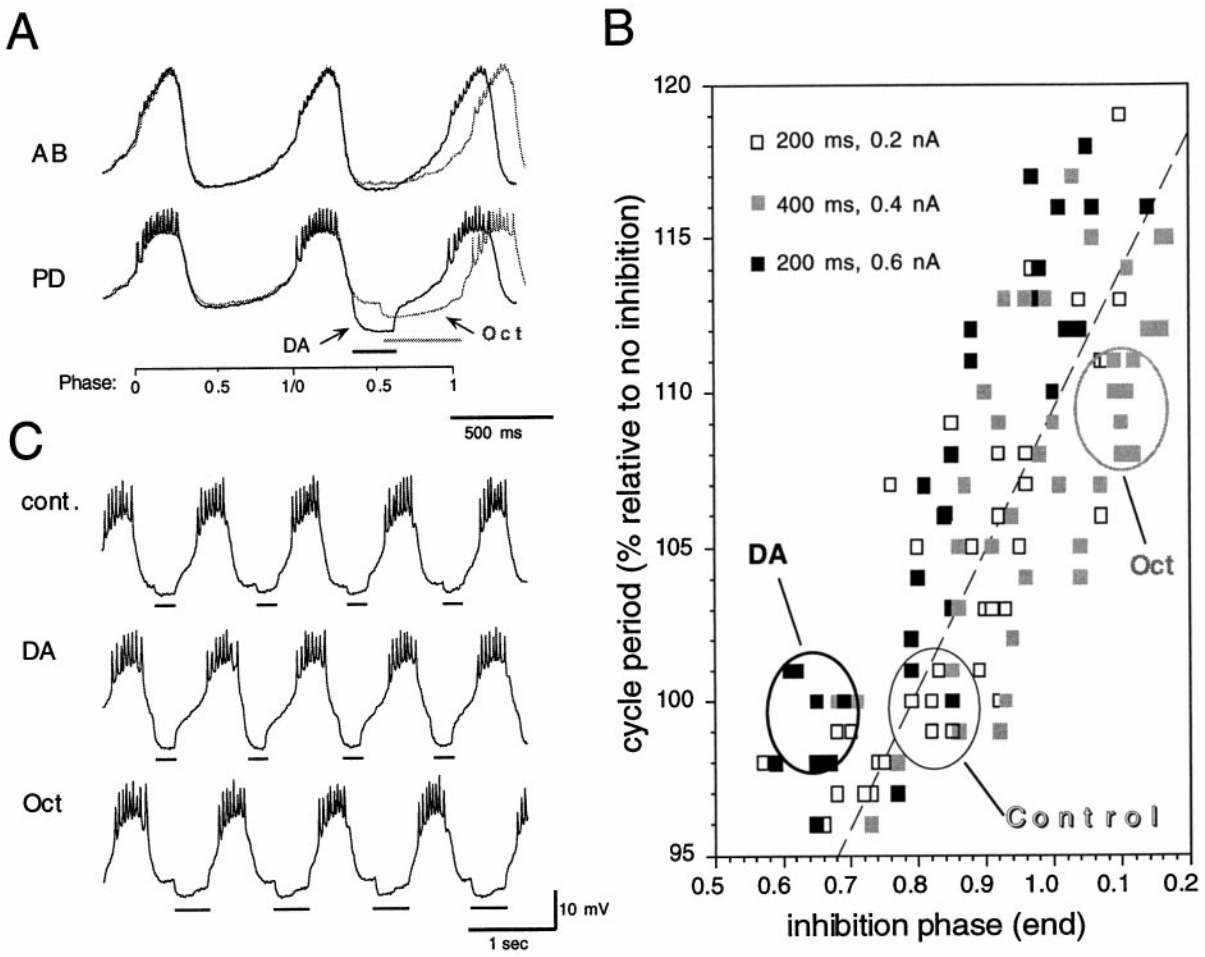

Figure 8. The effect of hyperpolarizing current injections to the PD neurons in an intact pyloric network with the LP → PD synapse pharmacologically blocked. In all the experiments shown, hyperpolarizing current pulses were intracellularly injected to a PD neuron while the neuron's membrane potential was recorded with a second electrode. *A*, Simultaneous recording from PD and AB neurons. Two sweeps (from the same preparation) are overlaid. In both, a cycle with no current injection is followed by one with an inhibitory stimulus mimicking the LP inhibition of PD during DA (*black*) or Oct (*gray*) (for details, see Results). The time of current injection is shown by the *black* and *gray bars*, and the phase of two cycles is shown based on the prestimulation cycle (the first spike in the AB neuron is defined as phase 0). *B*, The effect of inhibitory stimulation of PD on the pyloric cycle period. Single stimuli (three different stimulus protocols as shown in the graph's legend) were given at different phases along the PD bursting cycle. The stimuli duration and intensity correspond to those generated by the LP neuron in a fully intact network in control (*open squares*), DA (*black squares*), or Oct (*gray squares*) conditions. The phase of the end of the inhibitory stimulus (calculated relative to the preceding cycle with no stimulus as shown in *A*) is plotted against the change in cycle period generated by the inhibition (period with inhibition/period in previous cycle with no inhibition × 100). The end phase could exceed 1.0, as for example in the sweep marked Oct in *A*. Data points from four different preparations are shown. The *dashed line* is a linear fit calculated for all the data points shown (pooled together). The *oval* marked *Control* refers to the open data points, corresponding to LP inhibition of PD in a fully intact network in control conditions. Similarly, the areas marked *DA* and *Oct* refer to the *filled black* and *filled gray* data points, respectively, and represent LP inhibition of PD during DA or Oct bath application. *C*, The effect of repetitive inhibitory inputs to the PD neuron on the pyloric rhythm. The three PD traces (from the same neuron) show the effect of control- (*cont.*), DA-, and Oct-like repetitive inhibitory stimulation using stimulus parameters and phasing indicated by the *ovals* in *B*. The time of current injection is shown by the *bars*.

(mimicking Oct conditions) caused significant reduction in cycle frequency.

Our results suggest that the VD neuron plays little if any role in the amine modulation of pyloric cycle frequency. Octopamine exerts a weak excitatory effect on the isolated VD neuron (Flamm and Harris-Warrick, 1986b). However, Oct enhances synaptic inhibition at the LP → VD synapse (Johnson et al., 1995), and the inhibition from the LP neuron was usually strong enough to significantly reduce or eliminate the VD neuron spiking altogether (Fig. 5*A*), suggesting a minor role for the VD neuron in shaping the Oct-induced cycle frequency. The VD neuron is directly inhibited by both DA and 5HT (Flamm and Harris-Warrick, 1986b), and it fired weakly or not at all during application of these amines (Fig. 5*A*). Hyperpolarization of the VD neuron did not change the cycle frequency in the presence of DA, 5HT, or Oct (data not shown).

Time and concentration dependence of DA effect on cycle frequency

As described above, DA's effect on the pyloric cycle frequency reflects a compromise between its opposing effects on the AB and PD neurons. We conducted a number of experiments to further characterize how the individual effects of DA on the properties of the AB and PD neurons contribute to the overall modulatory effects of DA as described in the previous sections. We again tested the isolated AB–PD subnetwork with blocked descending inputs (Fig. 9). Under these conditions there is no cycling, and the PD neuron fires tonically, generating EPSPs in the AB neuron.

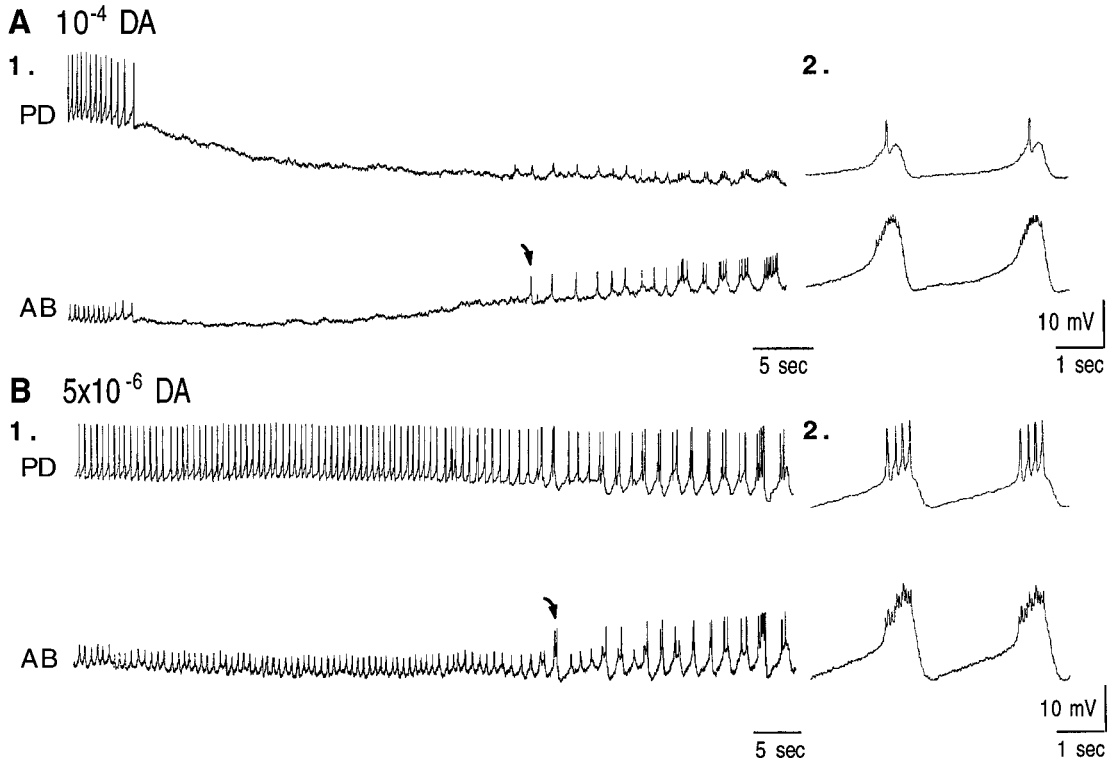

Figure 9. The onset of the effect of 10^{-4} M (*A*) or 5×10^{-6} M (*B*) dopamine bath application on an AB–PD subnetwork isolated from all pyloric and descending inputs. In both *A* and *B*, *panel 1* shows a 1 min period around the onset of dopamine's effect on the two neurons (the first AB spike is marked by an *arrow*). *Panel 2* shows the final and stable dopamine-induced rhythm (~5 min of bath application).

Figure 9*A* shows that during the initial entry of DA into the bath, the PD neuron responds earlier than the AB neuron. Approximately 15 sec passed after the beginning of the hyperpolarization of the PD neuron, before any sign of depolarization of the AB neuron was seen, and altogether 35 sec passed before the AB neuron was excited enough to fire its first action potential. Thus, DA's inhibition of the PD neuron has a significantly more rapid onset than DA's excitation of the AB neuron, and there is a definite time window when only the PD neuron inhibition is apparent, with no AB excitation. Similar results are seen with isolated AB and PD neurons: the onset of the PD response to DA is significantly more rapid than the AB response (data not shown). In the AB–PD subnetwork, can we also obtain DA excitation of the AB neuron with no PD neuron inhibition? Flamm and Harris-Warrick (1986b) showed that higher concentrations of DA (threshold 10^{-5} M) were needed to inhibit the PD neuron than to excite the AB neuron (10^{-6} M). As seen in Figure 9*B*, confirming these earlier findings, in the AB–PD subnetwork, 5×10^{-6} M DA was not sufficient to inhibit the PD neuron, but it did excite the AB neuron and generate rhythmic cycling. The lower DA concentration eventually produced a unique pattern, with no PD inhibition (Fig. 9*B2*). Thus by selecting time and dose combinations, we can isolate the inhibitory or the excitatory components of DA's effect on the AB–PD pacemaker subnetwork.

The experiment shown in Figure 10 further supports the idea of a balance between DA's two opposing effects on the AB and PD neurons, yielding a complex response at the subnetwork level. In this experiment, the PD neurons were eliminated one by one from an AB–2xPD network with intact descending inputs. DA was repeatedly bath-applied and washed out to test its effect on the 3, 2, and 1 pacemaker neuron group. When DA was applied to the AB–2xPD subnetwork, the major response was a transient reduction in cycle frequency, beginning at 1.5 min, which reversed by 4.5 min but did not exceed the initial cycle frequency. After photoinactivating one PD neuron, DA was applied to the AB–PD subnetwork; now the initial reduction in cycle frequency was only half as large and was shorter, replaced at 3.5 min by a marked 50% increase in cycle frequency. Finally, elimination of the second PD neuron yielded an isolated AB neuron, which responded to DA as usual with a delayed (3 min) twofold increase in cycle frequency. Thus, both the magnitude and duration of the inhibitory response to DA depends on the number of PD neurons electrically coupled to the AB pacemaker.

DISCUSSION

Effects of dopamine, serotonin, and octopamine on the pyloric cycle frequency

In this paper we demonstrate that the relative importance of each of the cellular components of the pyloric pacemaker in determining the final cycle frequency is not fixed but can vary under different modulatory conditions. Our approach has been to work our way up from single isolated AB and PD neurons to the isolated AB–PD and AB–2xPD subnetworks and finally to the intact network, determining the amine-induced cycle frequency at each step. To a first approximation, the effects of the three amines on the isolated AB, PD, and AB–PD groups were the same in the presence and absence of modulatory inputs from higher ganglia; thus, there are no obvious nonlinear interactions between the effects of each bath-applied amine and the descend-

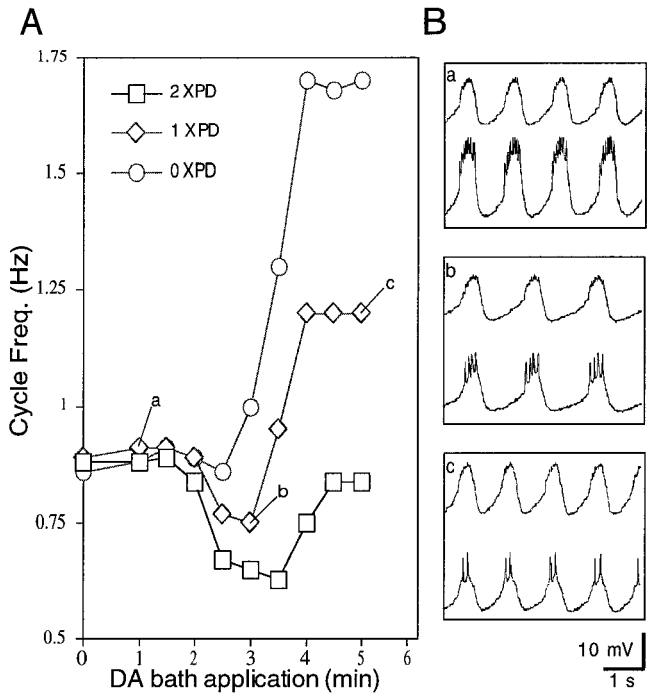

Figure 10. *A*, The biphasic effect of dopamine bath application (10^{-4} M) on the pyloric pacemaker subnetwork isolated from all pyloric synaptic inputs and with intact descending inputs. All the data were collected from a single preparation. Dopamine was bath-applied and washed before and after photoinactivation to sequentially remove the first and then the second PD neuron (AB–2xPD, AB–PD, and isolated AB). The *three panels in B* show simultaneous recording from the AB (*top traces*) and PD (*bottom traces*) neurons in the AB–PD subnetwork, at the time data points marked in *A* by corresponding letters.

ing modulatory inputs. Our comparison of amine effects on the components of the pyloric pacemaker group has illuminated our interpretation of how each amine determines the cycle frequency in the intact pyloric network.

One striking point that can be clearly seen in Figure 6 is that the order of amine efficacy in enhancing cycle frequency changes markedly with each level of complexity, from the isolated AB neuron to the intact network. Dopamine induces the highest cycle frequency in the isolated AB neuron, whereas 5HT and Oct equally generate the highest frequencies in the AB–PD and AB–2xPD subnetworks, and 5HT alone increases the cycle frequency in the intact network. These differences must reflect differing contributions of the different neurons and synapses to the final cycle frequency for each amine at each level of complexity.

In the presence of DA, the cycle frequency is strongly enhanced with the isolated AB neuron, weakly enhanced with the AB–PD subnetwork, and reduced below the control frequency with the AB–2xPD subnetwork and in the intact network. These results arise from the opposing effects of DA on the pacemaker AB and PD neurons (Fig. 2) (Eisen and Marder, 1984; Flamm and Harris-Warrick, 1986b). Recent work has shown that the PD neuron inhibition is accompanied by a conductance increase attributable to enhancement of I_A and $I_{K(Ca)}$ (Kloppenburg et al., 1999). The leaky, hyperpolarized PD neurons impose a marked electrical drag on the excited AB neuron, and this drag is greater when two PD neurons are present. Hooper and Marder (1987) observed a similar effect of proctolin on pyloric cycle frequency that varied with the number of PD neurons present. In their study, proctolin directly accelerated the AB neuron, whereas the PD neurons were unaffected by proctolin. In the presence of DA, it appears that the synaptic input to the AB–PD pacemaker kernel from the LP and VD neurons plays no significant role in determining the final DA-induced cycle frequency. This is despite the fact that DA strongly excites the LP neuron (Flamm and Harris-Warrick, 1986b; Harris-Warrick et al., 1995a) and enhances LP inhibition of the PD neurons (Johnson et al., 1995). The quantitative effect of DA on LP activity provides an explanation for this result. In addition to exciting the LP neuron, DA evokes a significant phase advance of the onset of the LP burst, attributable to a reduction in I_A and an enhancement of I_h (Harris-Warrick et al., 1995a). The LP burst duration is not prolonged because DA also excites and phase advances the PY neurons, which inhibit and terminate the LP burst (Harris-Warrick et al., 1995b). The phase of LP inhibition of PD is therefore advanced into a "refractory" region of the oscillatory cycle where the AB and PD neurons are just beginning to recover from their own burst-induced hyperpolarization. As we have shown (Figs. 7, 8), the additional LP inhibition at this phase has no net effect on the time for AB–PD repolarization to resume firing. The VD neuron is inhibited and hyperpolarized by DA, in part because of an increase in I_A (J. Peck and R. Harris-Warrick, unpublished data). The electrical synapses between the VD neuron and the pacemaker neurons are weakened by DA, and in addition they rectify such that hyperpolarization of the inhibited VD does not effectively hyperpolarize the AB or PD neurons (Fig. 1) (Johnson et al., 1993). In conclusion, the DA-evoked cycle frequency is dominated by DA's opposing effects on the pacemaker AB and PD neurons, with no contribution from the follower cells.

The cycle enhancement seen with 5HT results primarily from its direct effects on the AB pacemaker, with little contribution from either the PD or the follower neurons. 5HT enhances bursting in the isolated AB neuron [by a different ionic mechanism than DA (Harris-Warrick and Flamm, 1987)] but has no detectable effect on the PD neurons (Fig. 2) (Eisen and Marder, 1984; Flamm and Harris-Warrick, 1986b). Thus, the effects of 5HT on the cycle frequency of the isolated AB neuron, the AB–PD, and AB–2xPD subnetworks are virtually identical (Fig. 6). As with DA, the VD and LP neurons appear to play no role in 5HT's effects on the cycle frequency. The VD neuron is inhibited by 5HT and usually is silent; its hyperpolarization is not passed electrotonically to the AB/PD neurons because of the rectifying nature of these electrical synapses (Johnson et al., 1993). 5HT also directly inhibits the LP and weakens the synapses between the LP and the PD neurons (Johnson et al., 1995). As a consequence, LP inhibits the PD neurons to a lesser degree. Thus, the effect of 5HT on the cycle frequency of the intact pyloric network is the same as that seen in the isolated AB neuron and AB–PD pacemaker neurons.

An opposite conclusion can be drawn for Oct's control of cycle frequency, where feedback from the follower cells, in particular the LP neuron, plays a dominant role in determining the final cycle frequency of the intact pyloric network. Octopamine's enhancement of the cycle frequency of the isolated, cycling AB neuron is relatively modest (Fig. 3*B*) (Flamm and Harris-Warrick, 1986b) and is caused by a different ionic mechanism for burst enhancement than either DA or 5HT (Harris-Warrick and Flamm, 1987). However, Oct also slightly excites the isolated PD neuron (Fig. 2) (Flamm and Harris-Warrick, 1986b), which the other amines do not do. This is sufficient to make the Oct-induced

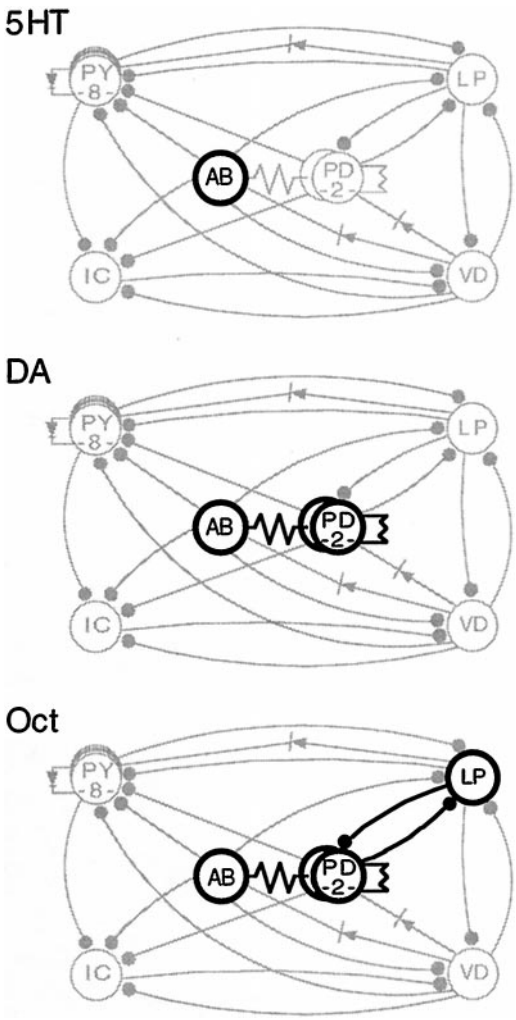

Figure 11. The pyloric network components that are the major targets of monoamine modulation of cycle frequency. Schematic diagrams of the intact pyloric network are shown. In each panel (*5HT*, *DA*, and *Oct*) the circuit components that are instrumental in determining the specific amine-induced cycle frequency are highlighted.

AB–PD and AB–2xPD subnetworks' cycle frequencies comparable to or even slightly higher than the 5HT-evoked frequencies (Figs. 4, 6) and significantly greater than the DA-evoked frequency. However, when we progress to the intact pyloric network, this accelerating effect of Oct is lost, and Oct has virtually no effect on the cycle frequency (Figs. 5, 6). As we have shown [see also Flamm and Harris-Warrick (1986a,b)], Oct prolongs and enhances spike activity of the LP neuron but does not enhance PY activity in the intact network as DA does. Thus, the LP neuron fires for a much longer fraction of the cycle than under control conditions. During this time, LP is inhibiting the PD neuron (and thus, electrotonically, the AB neuron); in addition, the strength of the LP → PD inhibitory synapse is also enhanced by Oct (Johnson et al., 1995). This prolonged and strengthened inhibition delays the pacemaker group from repolarizing to fire their next burst. As a consequence, the overall cycle frequency is not accelerated and sometimes even slowed (Fig. 5*A*) despite Oct's excitation of both the AB and PD neurons in the pacemaker subnetwork. The VD neuron is directly but weakly excited by Oct (Flamm and Harris-Warrick, 1986b). However, it does not become active during Oct application in the intact network because of strong inhibition by the activated LP neuron, so it does not contribute to setting the cycle frequency.

Time and concentration dependence of DA effect on cycle frequency

Our work also shows that DA has a complex time- and concentration-dependent effect on the AB–PD subnetwork cycle frequency. At high concentrations (10^{-4} M), DA evokes a transient reduction in cycle frequency followed by a recovery to near control cycle frequency under steady-state conditions (Figs. 6, 9, 10). The early deceleration is caused by DA inhibition of the PD neuron, whereas the later acceleration is caused by the DA's delayed enhancement of AB bursting. It was been shown previously (Flamm and Harris-Warrick, 1986b), and confirmed here (Fig. 9), that the threshold for PD inhibition by DA (10^{-5} M) is higher than for AB excitation (10^{-6} M), so the observed results cannot be caused by the slowly rising concentration of DA in our bath. Indeed, this would have led to an early enhancement of cycling followed by a later reduction, the opposite of what is seen. We are left with several hypotheses to explain this result. First, the second messenger mechanisms leading to PD inhibition could be activated more rapidly than those leading to AB excitation. Alternatively, there could be a difference in the DA receptor level between the AB and PD neurons; more receptors in the PD neurons could facilitate a more rapid response. Finally, the DA receptors on the PD neurons might be localized to be more readily accessible to bath-applied DA than those on the AB neuron. Unfortunately, no evidence is available to distinguish between these mechanisms.

There are several possible consequences of these different time- and concentration-dependent effects of DA. If the modulatory neurons providing DA to the STG were to fire weakly, only a low concentration of DA would be seen in the ganglion, and this could evoke an acceleration in AB cycle frequency without inhibition of the PD neurons, as seen in Figure 9*B*. Brief higher firing rates might evoke just the PD-dependent reduction in firing frequency seen early during bath application of DA. Finally, prolonged high firing rates would lead to the biphasic effect seen in Figure 9*A*, with the PD neurons inhibited throughout. All of these responses can be seen in the dish with local pressure ejection of pulses of DA from a pipette (data not shown). Because the PD neurons are motoneurons controlling dilation of the pyloric valve, the ability to independently affect the cycle frequency and the spike frequency of the PD neurons (and thus activation of the dilator muscles) will allow greater flexibility in motor output.

Conclusion

Our results show the complexity of the neuronal interactions that lead to the modulatory control of cycle frequency in the pyloric network. As summarized in Figure 11, the major circuit components that are instrumental in setting the cycle frequency vary depending on the modulatory conditions, from the predominant role of the single AB neuron in 5HT to the AB–PD pacemaker subnetwork in DA and the AB–PD–LP subnetwork in Oct. Although the AB neuron is universally believed to be the most important pacemaker in the pyloric network, we cannot predict the monoamine effects on the pyloric network frequency based solely on their effects on the isolated AB neuron. By having contrasting effects on the PD neurons (DA inhibits, 5HT has no effect, and Oct excites), the amines can dramatically modify their net effects on the AB–PD group. In addition, the pacemaker

group does not exist in a vacuum; the amines' different effects on both the LP neuron and its synapse onto the PD neurons shape the extent to which this input is relevant in controlling the pacemaker group's cycle frequency. Finally, by differentially modulating the PY neurons' inhibition of the LP neuron, DA and Oct impart very different roles to the LP neuron in the control of cycle frequency.

These results emphasize that the effects of a neuromodulator on a network cannot be predicted simply from the sum of the modulator effects on each of the component neurons in isolation: the network generates complex and nonlinear interactions that must be taken into account as well. However, by carefully studying the different components both alone and in varying combinations, the general mechanisms of frequency control can be determined.

REFERENCES

Abbott LF, Marder E, Hooper SL (1991) Oscillating networks: control of burst duration by electrically coupled neurons. Neural Comput 3:487–497.

Ayali A, Harris-Warrick RM (1998) Combined effects of amine modulation and CPG network interactions in the lobster stomatogastric ganglion. Brain Res 794:155–161.

Ayali A, Johnson BR, Harris-Warrick RM (1998) Dopamine modulates graded and spike-evoked synaptic inhibition independently at single synapses in pyloric network of lobster. J Neurophysiol 79:2063–2069.

Baro DJ, Levini RM, Kim MT, Willms AR, Cole CL, Rodriguez HE, Harris-Warrick RM (1997) Quantitative single-cell–reverse transcription-PCR demonstrates that A-current magnitude varies as a linear function of shal gene expression in identified stomatogastric neurons. J Neurosci 17:6597–6610.

Bidaut M (1980) Pharmacological dissection of pyloric network of the lobster stomatogastric ganglion using picrotoxin. J Neurophysiol 44:1089–1101.

Dickinson PS, Mecsas C, Marder E (1990) Neuropeptide fusion of two motor pattern generator circuits. Nature 344:155–158.

Eisen JS, Marder E (1982) A mechanism underlying pattern generation in lobster stomatogastric ganglion as determined by selective inactivation of identified neurons. III. Synaptic connections of electrically coupled pyloric neurons. J Neurophysiol 48:1392–1415.

Eisen JS, Marder E (1984) A mechanism for the production of phase shifts in a pattern generator. J Neurophysiol 51:1375–1393.

Flamm RE, Harris-Warrick RM (1986a) Aminergic modulation in lobster stomatogastric ganglion. I. Effects on motor pattern and activity of neurons within the pyloric circuit. J Neurophysiol 55:847–865.

Flamm RE, Harris-Warrick RM (1986b) Aminergic modulation in lobster stomatogastric ganglion. II. Target neurons of dopamine, octopamine, and serotonin within the pyloric circuit. J Neurophysiol 55:866–881.

Getting PA (1989) Emerging principles governing the operation of neural networks. Annu Rev Neurosci 12:185–204.

Harris-Warrick RM, Flamm RE (1986) Chemical modulation of a small central pattern generator circuit. Trends Neurosci 9:432–437.

Harris-Warrick RM, Flamm RE (1987) Multiple mechanisms of bursting in a conditional bursting neuron. J Neurosci 7:2113–2128.

Harris-Warrick RM, Marder E (1991) Modulation of neural networks for behavior. Annu Rev Neurosci 14:39–57.

Harris-Warrick RM, Coniglio LM, Barazangi N, Guckenheimer J, Gueron S (1995a) Dopamine modulation of transient potassium current evokes phase shifts in a central pattern generator network. J Neurosci 15:342–358.

Harris-Warrick RM, Coniglio LM, Levini RM, Gueron S, Guckenheimer J (1995b) Dopamine modulation of two subthreshold currents produces phase shifts in activity of an identified motoneuron. J Neurophysiol 74:1404–1420.

Hartline DK, Graubard K (1992) Cellular and synaptic properties in the crustacean stomatogastric nervous system. In: Dynamic biological networks: the stomatogastric nervous system (Harris-Warrick RM, Marder E, Selverston AI, Moulins M, eds), pp 31–86. Cambridge, MA: MIT.

Hooper SL, Marder E (1987) Modulation of the lobster pyloric rhythm by the peptide proctolin. J Neurosci 7:2097–2112.

Johnson BR, Harris-Warrick RM (1990) Aminergic modulation of graded synaptic transmission in the lobster stomatogastric ganglion. J Neurosci 10:2066–2076.

Johnson BR, Harris-Warrick RM (1997) Amine modulation of glutamate response from pyloric motor neurons in the lobster stomatogastric ganglion. J Neurophysiol 3210–3221.

Johnson BR, Hooper SL (1992) Overview of the stomatogastric nervous system. In: Dynamic biological networks: the stomatogastric nervous system (Harris-Warrick RM, Marder E, Selverston AI, Moulins M eds), pp 1–30. Cambridge, MA: MIT.

Johnson BR, Peck JH, Harris-Warrick RM (1993) Amine modulation of electrical coupling in the pyloric network of the lobster stomatogastric ganglion. J Comp Physiol [A] 172:715–732.

Johnson BR, Peck JH, Harris-Warrick RM (1995) Distributed amine modulation of graded chemical transmission in the pyloric network of the lobster stomatogastric ganglion. J Neurophysiol 74:437–452.

Katz PS (1999) Beyond neurotransmission: neuromodulation and its importance for information processing. Oxford: Oxford UP, in press.

Kepler TB, Marder E, Abbott LF (1990) The effect of electrical coupling on the frequency of model neuronal oscillators. Science 248:83–85.

Kloppenburg P, Levini RM, Harris-Warrick RM (1999) Dopamine modulates two potassium currents and inhibits the intrinsic firing properties of an identified motoneuron in a central pattern generator network. J Neurophysiol 81:29–38.

Marder E (1984) Roles for electrical coupling in neural circuits as revealed by selective neuronal deletions. J Exp Biol 112:147–167.

Marder E, Skiebe P, Christie AE (1994) Multiple modes of network modulation. Verh Dtsch Zool Ges 87:177–184.

Miller JP (1987) Pyloric mechanisms. In: The crustacean stomatogastric system (Selverston AI, Moulins M, eds), pp 109–136. Berlin: Springer.

Miller JP, Selverston AI (1979) Rapid killing of single neurons by irradiation of intracellularly injected dye. Science 206:702–704.

Miller JP, Selverston AI (1982a) Mechanisms underlying pattern generation in lobster stomatogastric ganglion as determined by selective inactivation of identified neurons. II. Oscillatory properties of pyloric neurons. J Neurophysiol 48:1378–1391.

Miller JP, Selverston AI (1982b) Mechanisms underlying pattern generation in lobster stomatogastric ganglion as determined by selective inactivation of identified neurons. IV. Network properties of pyloric system. J Neurophysiol 48:1416–1432.

Mulloney B, Selverston AI (1974) Organization of the stomatogastric ganglion in the spiny lobster. I. Neurons driving the lateral teeth. J Comp Physiol 91:1–32.

Nagy F, Miller JP (1987) Pyloric pattern generation in *Panulirus interruptus* is terminated by blockade of activity through the stomatogastric nerve. In: The crustacean stomatogastric system (Selverston AI, Moulins M, eds), Appendix A, pp 136–139. Berlin: Springer.

Russell DF (1979) CNS control of pattern generation in the lobster stomatogastric ganglion. Brain Res 177:598–602.

Selverston AI, Miller JP (1980) Mechanisms underlying pattern generation in lobster stomatogastric ganglion as determined by selective inactivation of identified neurons. I. Pyloric system. J Neurophysiol 44:1102–1121.

Selverston AI, King DG, Russell DF, Miller JP (1976) The stomatogastric nervous system: structure and function of a small neural network. Prog Neurobiol 7:215–290.

Selverston AI, Panchin YV, Arshavski YI, Orlovsky GN (1998) Shared features of invertebrate central pattern generators. In: Neurons, networks, and motor behavior (Stein SG, Grillner S, Selverston AI, Stuart DG, eds), pp 105–118. Cambridge, MA: MIT.

Sharp A, Abbott LF, Marder E (1992) Artificial electrical synapses in oscillatory neurons. J Neurophysiol 67:1691–1694.

Sillar KT, Kiehn O, Kudo N (1998) Chemical modulation of vertebrate motor circuits. In: Neurons, networks, and motor behavior (Stein SG, Grillner S, Selverston AI, Stuart DG, eds), pp 183–194. Cambridge, MA: MIT.

Stein SG, Grillner S, Selverston AI, Stuart DG (1998) Neurons, networks, and motor behavior. Cambridge, MA: MIT.